



Original Article

Sodium-Glucose Cotransporter-2 Inhibitor Enhances Hepatic Gluconeogenesis and Reduces Lipid Accumulation via AMPK-SIRT1 Activation and Autophagy Induction

Si Woo Lee¹, Hyunki Park², Minyoung Lee³, Hyangkyu Lee², Eun Seok Kang^{1,3,4,5}

Graduate School of Medicine, Yonsei University; Department of Clinical Nursing Science, Yonsei University College of Nursing; ³Department of Internal Medicine, Yonsei University College of Medicine; ⁴Severance Hospital Diabetes Center; ⁵Institute of Endocrine Research, Yonsei University College of Medicine, Seoul, Korea

Background: Sodium-glucose cotransporter type 2 (SGLT2) inhibitors, such as dapagliflozin, are primarily used to lower glucose in type 2 diabetes. Recent studies suggest broader metabolic effects, particularly in the liver. This study explores the molecular mechanisms by which dapagliflozin influences hepatic glucose and lipid metabolism, hypothesizing that it activates the 5'-adenosine monophosphate-activated protein kinase (AMPK)-sirtuin 1 (Sirt1) pathway to promote gluconeogenesis and reduce lipid accumulation via autophagy.

Methods: HepG2 hepatocellular carcinoma cells were treated with dapagliflozin, and Western blotting, quantitative reverse transcription polymerase chain reaction, and fluorescence microscopy were used to assess gluconeogenic enzyme expression and autophagy. In vivo, mice with liver-specific autophagy related 7 (Atg7) deletion and those on a high-fat diet were used to evaluate glucose regulation, lipid metabolism, and autophagy.

Results: Dapagliflozin significantly increased expression of gluconeogenic enzymes like phosphoenolpyruvate carboxykinase (PEPCK) in HepG2 cells and enhanced autophagic flux, evidenced by increased light chain 3B (LC3B)-II levels and autophagosome formation. AMPK-Sirt1 activation was confirmed as the underlying mechanism. Additionally, dapagliflozin reduced fatty acid synthesis by suppressing enzymes such as acetyl-CoA carboxylase and fatty acid synthase, while promoting fatty acid degradation via carnitine palmitoyltransferase 1a (CPT1a) upregulation. In high-fat diet mice, dapagliflozin increased hepatic gluconeogenesis and reduced lipid accumulation, though serum cholesterol and triglyceride levels were unaffected.

Conclusion: Dapagliflozin enhances hepatic gluconeogenesis and reduces steatosis by activating the AMPK-Sirt1 pathway and promoting autophagy. These findings suggest that SGLT2 inhibitors could offer therapeutic benefits for managing hepatic lipid disorders, beyond glycemic control.

Keywords: Dapagliflozin; Gluconeogenesis; Glycemic control; Non-alcoholic fatty liver disease

Received: 25 October 2024, Revised: 31 December 2024,

Accepted: 12 February 2025

Corresponding author: Eun Seok Kang

Division of Endocrinology and Metabolism, Department of Internal Medicine, Yonsei University College of Medicine, 50-1 Yonsei-ro, Seodaemun-gu, Seoul 03722, Korea

Tel: +82-2-2228-1968, Fax: +82-2-393-6884, E-mail: edgo@yuhs.ac

Copyright © 2025 Korean Endocrine Society

This is an Open Access article distributed under the terms of the Creative Commons Attribution Non-Commercial License (https://creativecommons.org/ licenses/by-nc/4.0/) which permits unrestricted non-commercial use, distribution, and reproduction in any medium, provided the original work is properly cited.

INTRODUCTION

Sodium-glucose cotransporter type 2 (SGLT2) inhibitors represent a significant advancement in glucose-lowering therapies, primarily blocking renal glucose reabsorption and thereby reducing blood glucose levels [1,2]. Dapagliflozin (DAPA), a known SGLT2 inhibitor, is widely approved for managing type 2 diabetes mellitus owing to its efficacy in impeding SGLT2-dependent renal glucose reabsorption [3]. In addition, DAPA aids in weight reduction, decreases cardiovascular mortality, and potentially slows the progression of diabetic kidney disease [4]. Beyond their core role in glycemic control, SGLT2 inhibitors have garnered substantial interest for their ancillary benefits, including the alleviation of body fluid overload through osmotic diuresis, which in turn reduces blood pressure and improves heart failure outcomes [5-12]. These cardiovascular benefits have accelerated the clinical adoption of SGLT2 inhibitors [4,9-11]. Nevertheless, further investigation of their metabolic effects on other tissues is essential to optimize their therapeutic potential and ensure comprehensive clinical safety.

SGLT2 inhibitors also enhance hepatic glucose production, which is often associated with elevated plasma glucagon levels [13]. The exact mechanism behind SGLT2-induced gluconeogenesis remains debated, with some research suggesting an indirect effect via increased urinary glucose excretion, while others proposing a direct impact on pancreatic alpha cells, thereby stimulating glucagon secretion [14,15]. In addition, SGLT2 inhibitors reduce hepatic steatosis by promoting fatty acid oxidation and suppressing lipogenesis [16-18]. Despite these findings, the specific molecular mechanisms through which SGLT2 inhibitors influence hepatic glucose and lipid metabolism have not been completely clarified.

Thus, this study aimed to elucidate the molecular pathways that explained the influence of SGLT2 inhibitors on liver lipid and glucose metabolism. Specifically, we examined the role of the activation of 5'-adenosine monophosphate-activated protein kinase (AMPK) and hepatic autophagy, both crucial for maintaining hepatic glucose and lipid homeostasis [19,20]. We hypothesized that SGLT2 inhibitors stimulated hepatic gluconeogenesis and reduced hepatic lipid accumulation by activating AMPK and enhancing hepatic autophagy. To test this hypothesis, we employed a comprehensive approach incorporating both *in vitro* and *in vivo* experiments using HepG2 cells and a mouse model of hepatic autophagy deficiency (liver-specific autophagy related 7 [Atg7] knockout mice).

METHODS

Animal experiments

Four-week-old male C57BL/6J mice were housed in a controlled environment with a 12-hour light/dark cycle and temperatures maintained at 21°C±2°C and humidity at 60%±10%. After a 1-week acclimation period, the mice were assigned to four groups based on their diet and treatment: (1) standard chow diet; (2) standard chow diet supplemented with DAPA (2.0 mg/kg/ day) mixed into the food pellets; (3) high-fat diet (HFD; 60% kcal from fat; D12492; Research Diets Inc., New Brunswick, NJ, USA); and (4) HFD with DAPA (2.0 mg/kg/day) incorporated into the food pellets. Liver-specific Atg7 knockout (Atg7Δhep) mice were provided with an HFD with or without DAPA treatment (2.0 mg/kg/day) mixed into their food pellets. To create liver-specific Atg7-deficient mice, Atg7^{f/f} mice were bred with Cre mice driven by the albumin promoter, resulting in the generation of atg7^{f/f};alb-Cre mice (Atg7Δhep). Five-week-old mice were placed on diet rich in fats (n=37) for 8 weeks before administration of the drug. Age-matched control group mice were given a standard chow diet (negative control) (n=12).

Following a 12-week period, the chow-fed mice were categorized into two groups: one receiving chow (n=6) and the other receiving chow+DAPA (n=6). The HFD-induced diabetic mice were also divided into two cohorts: HFD (n=18) and HFD+DAPA (n=19). Treatment continued for an additional 12 weeks, during which blood glucose concentrations, body weight, and food consumption were assessed weekly. Following the treatment phase, the mice were administered with tiletamine–zolazepam (Zoletil; 50 mg/kg; Virbac, Carros, France). Serum samples were obtained and preserved at -80°C, while hepatic tissues were harvested, flash frozen in liquid nitrogen, and maintained at -80°C until subsequent analysis.

All animal experiments were approved by the Institutional Animal Care and Use Committee at Yonsei University College of Medicine (approval number: 2024-0056) and were conducted in compliance with applicable guidelines and regulations

Western blotting

Both cells and liver tissues were lysed using radioimmunoprecipitation assay (RIPA) buffer, which comprised 20 mM Tris-HCl (pH 7.5), 150 mM NaCl, 1 mM ethylenediaminetetraacetic acid, 1 mM egtazic acid, 1% ethoxylated nonylphenol, 1% sodium deoxycholate, 2.5 mM sodium pyrophosphate, 1 mM β -glycerophosphate, 1 mM sodium vanadate, and 1 $\mu g/mL$ leupeptin (BRI-9010-010M, Tech & Innovation Co. Ltd., Chun-

cheon, Korea), using a mixture of protease and phosphatase inhibitors (78440, Thermo Scientific, Waltham, MA, USA). Protein samples were separated using 10% and 15% polyacrylamide gels, followed by transfer to polyvinylidene fluoride membranes (PVH00010, Millipore, Burlington, MA, USA) and nitrocellulose membranes. To assess the levels of various proteins, the membranes were treated with primary antibodies, including phosphoenolpyruvate carboxykinase (PEPCK; ab28455, Abcam, Cambridge, UK), glucose 6-phosphatase (G6Pase; ab83690, Abcam), light chain 3B (LC3B) (L7543, Sigma-Aldrich, St. Louis, MO, USA), AMPK (2532S, Cell Signaling, Danvers, MA, USA), p-AMPK (2535S, Cell Signaling), actin beta (ACTB) (A1978, Sigma-Aldrich), and an horseradish peroxidase-conjugated anti-mouse immunoglobulin G (IgG) (7076S, Cell Signaling). For the secondary antibody, anti-rabbit IgG (7074S, Cell Signaling) was utilized.

RNA extraction and quantitative reverse transcription polymerase chain reaction

Total RNA was extracted from HepG2 cells using TRIzol according to the manufacturer's protocol. RNA purity and concentration were assessed using a NanoDrop spectrophotometer by measuring absorbance at 260/280 nm. For cDNA synthesis, the Prime-ScriptTM RT Reagent Kit (Perfect Real-Time) (Cat. #RR037A, Takara Bio, Kusatsu, Japan) was used according to the manufacturer's instructions. Quantitative real-time polymerase chain reaction (PCR) was performed using the TB Green premix Ex Taq (RR420A, Takara Bio) in a qPCR machine (CronoSTAR™ 96 Real-Time PCR System, Takara Bio) to measure the expression levels of the target genes glucose-6-phosphatase (G6PC), phosphoenolpyruvate carboxykinase 1 (PCK1), pyruvate kinase liver type (PKLR), sirtuin 1 (SIRT1), fatty acid synthase (FAS), acetyl-CoA carboxylase (ACC), carnitine palmitoyltransferase 1α (CPT1α), hydroxyacyl-CoA dehydrogenase trifunctional multienzyme complex subunit alpha (HADHa), long-chain acyl-CoA dehydrogenase (LCAD), and peroxisome proliferator-activated receptor alpha (PPARα). Gene-specific primers were designed based on sequences obtained from the National Center for Biotechnology Information nucleotide database. The thermal cycling conditions were as follows: initial denaturation at 95°C for 30 seconds, followed by 40 cycles of 95°C for 5 seconds and 60°C for 30 seconds. Relative gene expression levels were calculated using the ΔΔCt method, normalizing to glyceraldehyde 3-phosphate dehydrogenase.

Assessment of autophagic flux using fluorescence microscopy

HepG2 cells were transfected for 48 hours with a plasmid that encoded a green fluorescent protein (GFP)-tagged microtubule-associated protein 1 light chain 3 and monomeric red fluorescent proteins (mRFP) combined with GFP and LC3 using lipofectamine 2000 (1166-027, Invitrogen, Waltham, MA, USA). After transfection, the cells were fixed in a solution of 4% paraformaldehyde (PFA) in phosphate buffer (pH 7.4) for 10 minutes. Following fixation, the cells were washed three times using phosphate-buffered saline (PBS) for 5 minutes each time and then analyzed using an LSM 700 confocal microscope (Carl Zeiss, Oberkochen, Germany).

Cell maintenance and experimental procedures

Hepatocarcinoma cell line (HepG2) cells were grown in Dulbecco's modified Eagle's medium (SH30243.01, Thermo Scientific) under 5% CO2 conditions in a 37°C incubator. The medium was supplemented with 10% fetal bovine serum (SH30071.03, Thermo Scientific) and 1% each of penicillin and streptomycin (SV30010, Thermo Fisher Scientific). HepG2 cells were pre-incubated with bafilomycin A1 (Baf A1) (B1793, Sigma-Aldrich) or chloroquine (C6628, Sigma-Aldrich) for 2 hours then treated with DAPA (10 μ M) for 12 hours. Hepatic cells were exposed to 250 μ M palmitic acid (PA) along with DAPA (10 μ M) for 24 hours to establish an *in vitro* system simulating hepatic lipid accumulation.

Tests for oral glucose, insulin, and pyruvate tolerance

For the oral glucose tolerance test (OGTT), mice were made to fast overnight and then received an oral gavage of 40% glucose solution at a dosage of 2 g/kg body weight. Blood glucose levels were assessed at baseline and then again at 30, 60, 90, and 120 minutes during the test. Insulin tolerance tests were performed after a 4-hour fasting period, during which insulin (0.75 units/kg; catalogue number 9177C, Sigma-Aldrich) was given via intraperitoneal injection, and blood glucose measurements were taken according to the previously outlined method. At the time of the pyruvate tolerance test (PTT), mice were given an intraperitoneal injection of sodium pyruvate (2 g/kg; catalogue number P2256, Sigma-Aldrich) mixed in PBS after an 18-hour fast. Following the injection, blood samples were obtained from the tail vein. Blood glucose levels were measured using an Accu-Chek Performa glucometer (Bioehringer-Mannheim, Indianapolis, IN, USA).



Glucose production assay

Glucose synthesis from cells was evaluated with a colorimetric detection kit for glucose (K606-100, BioVision, Milpitas, CA, USA), as per the manufacturer's specifications. In summary, HepG2 cells were exposed to DAPA for 12 hours, either in its presence or absence. The prepared conditioned medium was subsequently gathered and combined with the reaction solution, then incubated at room temperature for 30 minutes. Absorbance was measured at 450 nm with a 96-well plate reader (Molecular Devices, Sunnyvale, CA, USA).

Haematoxylin and eosin staining

Liver tissues were preserved using 4% PFA, embedded in paraffin, and subjected to H&E staining. Lipid buildup was examined through electron microscopy.

Electron microscopy for transmission imaging

Transmission electron microscopy techniques was utilized to observe autophagic vacuoles in the liver. Mouse liver tissue, fixed with glutaraldehyde, was subjected to post-fixation using 2% osmium tetroxide and then dehydration through a series of alcohol solutions. Finally, it was flat embedded in EPON 812 (100503-876, Electron Microscopy Sciences, Hatfield, PA, USA). Ultrathin sections of 300 nm were created and examined using an electron microscope (JEM-1011, JEOL/Mega-View II, Olympus, Tokyo, Japan).

Analysis of serum lipid concentrations and hepatic steatosis

Blood serum samples were dispatched to the Department of Laboratory Animal Resources in Yonsei University College of Medicine for the evaluation of total triglyceride and cholesterol levels.

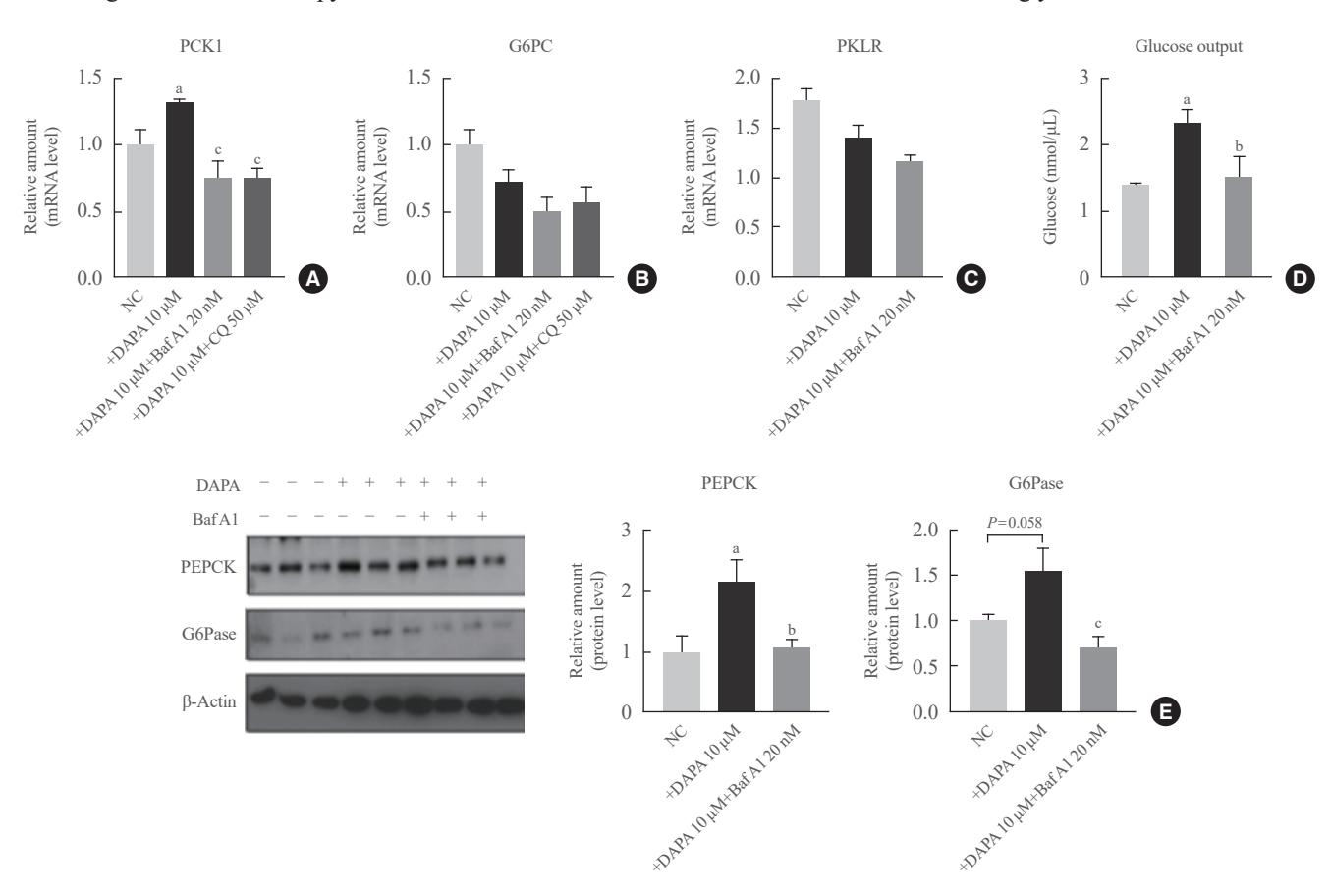


Fig. 1. Dapagliflozin (DAPA) increases autophagy-dependent glucose output and upregulates the levels of gluconeogenesis-related enzymes, whereas glycolytic enzymes remain unaffected in HepG2 cells. HepG2 cells are treated with DAPA (10 μM) and bafilomycin A1 (Baf A1; 20 nM) or chloroquine (CQ; 50 µM). Real-time quantitative reverse transcription polymerase chain reaction reveals that DAPA increases the expression of phosphoenolpyruvate carboxykinase 1 (PCK1) (A) but not that of glucose-6-phosphatase (G6PC) (B). However, DAPA has no significant effect on the mRNA expression of pyruvate kinase liver type (PKLR) (C) in HepG2 cells. DAPA treatment increases the glucose output (D). (E) Western blot analysis showing increased levels of PCK1 and G6PC, which encode gluconeogenic enzymes. Data are presented as the mean \pm standard error of the mean. PEPCK, phosphoenolpyruvate carboxykinase. Significance levels indicated as ${}^{a}P$ <0.05 when compared with negative control (NC); bP <0.05 when compared with DAPA group; cP <0.01 when compared with DAPA group.

Analysis of statistical data

Data are presented as the average ± standard error of the mean. Comparisons between two and three groups were performed using Student's *t* test and one-way or two-way analysis of variance (ANOVA) with Bonferroni's *post hoc* test, respectively. All statistical analyses were conducted using GraphPad Prism version 8 (GraphPad Software Inc., San Diego, CA, USA). A *P* value of

< 0.05 was considered statistically significant.

RESULTS

DAPA enhanced the expression of key rate-limiting enzymes associated with gluconeogenesis in HepG2 cells

To examine how DAPA influences hepatic gluconeogenesis, we

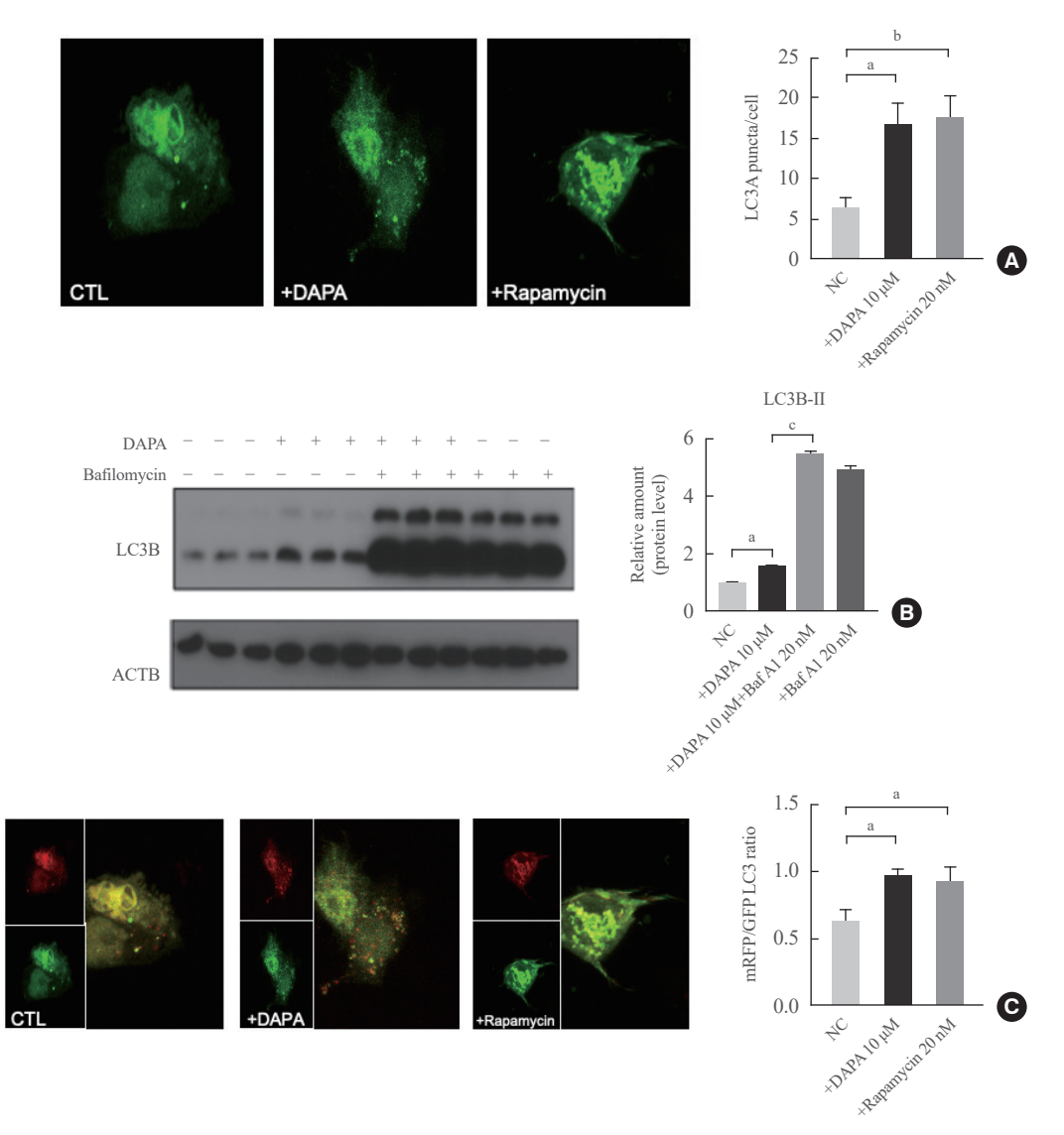


Fig. 2. Dapagliflozin (DAPA) stimulates autophagy in HepG2 cells. (A) Using the autophagy marker green fluorescent protein (GFP)-light chain 3A (LC3A), HepG2 cells are treated with DAPA ($10~\mu M$) for 12 hours. Fluorescent images are then captured using confocal microscopy ($63\times$ magnification). The histogram columns indicate the quantity of LC3A puncta per cell, with a minimum of 10 random fields selected from each sample. (B) Light chain 3B (LC3B)-II levels are increased in cells treated with DAPA, as indicated by Western blot analysis. In the group treated with bafilomycin A1 (Baf A1), DAPA triggers autophagic flux. (C) After transfecting hepatic cells with monomeric red fluorescent protein (mRFP)-GFP-LC3B, DAPA is given for of 12 hours. Fluorescent images are then captured using confocal microscopy ($63\times$ magnification). The GFP signals are unstable at low lysosomal pH, leading to its degradation. Conversely, red fluorescent protein signals remain more stable in acidic environments, thus retaining its red fluorescence. The histogram columns indicate the ratio of mRFP to GFP LC3B puncta. Data are presented as the mean \pm standard error of the mean. CTL, control; NC, negative control; ACTB, actin beta. Significance levels are indicated as follows: ${}^aP < 0.05$; ${}^bP < 0.001$; ${}^cP < 0.0001$.

investigated its impact on the levels of key enzymes related to gluconeogenic and glycolytic pathway in HepG2 hepatocellular carcinoma cells. Real-time quantitative reverse transcription polymerase chain reaction (qRT-PCR) analysis demonstrated that a 10-hour treatment with DAPA (10 µM) significantly increased the expression of the gluconeogenic enzyme PCK1 (soluble) (Fig. 1A), but it did not affect the expression of G6PC (catalytic subunit) (Fig. 1B). Correspondingly, we investigated PEPCK and G6Pase expression in HepG2 cells treated with DAPA (10 µM) for 12 hours. PEPCK and G6Pase protein levels were elevated, suggesting enhanced gluconeogenesis (Fig. 1E). In contrast, DAPA did not significantly alter the mRNA levels of PKLR (Fig. 1C). To determine whether the gluconeogenic effect of DAPA was mediated through autophagy, cells were cotreated with DAPA and Baf A1, a lysosomal inhibitor. Baf A1 treatment attenuated the DAPA-induced increase in PEPCK and G6Pase expression (Fig. 1E) and reduced glucose production (Fig. 1D). These findings indicate that DAPA specifically modulates the expression of gluconeogenic enzymes in HepG2 cells. Furthermore, they underscore the involvement of autophagy in mediating DAPA-induced gluconeogenesis.

DAPA triggered autophagic activity, resulting in increased levels of gluconeogenic enzymes

Given that autophagy enhanced gluconeogenesis in hepatic tissues [21], we investigated if DAPA enhanced autophagy in hepatocytes by introducing a vector into HepG2 cells that expressed the autophagy marker light chain 3A (LC3A), a microtubule-associated protein involved in autophagy conjugated with GFP. DAPA treatment increased the quantity of GFP-LC3A fluorescent puncta, indicating the presence of autophagosomes in the cytosolic space (Fig. 2A). In contrast, puncta were hardly noticeable in the control cells (Fig. 2A). To validate these findings, we conducted Western blot analysis, and the results revealed higher levels of LC-3B-II in the DAPA group than in the control group; this suggested that DAPA stimulated autophagy in hepatic cells (Fig. 2B). Cells were treated with Baf A1 to prevent autophagy, followed by DAPA treatment to assess whether the increase in LC3B levels induced by DAPA was due to autophagy activation or a blockage in autophagic flux. DAPA additionally elevated LC-3B-II levels in cells pretreated with Baf A1, indicating that DAPA promoted autophagy instead of inhibiting it (Fig. 2B). Next, hepatic cells were transfected with a tandem construct that encoded LC3 fused to both mRFP and GFP, allowing for the assessment of autophagic turnover.

GFP was broken down in the acidic environment of the lyso-

some, resulting in the disappearance of the green fluorescence. In contrast, red fluorescent signal remained stable in such conditions, preserving the red fluorescence. A yellow fluorescent signal, resulting from the combination of mRFP and GFP, was observed in autophagosomes, whereas only red signals (mRFP) were observed in autolysosomes. The quantity of red and yellow puncta was increased in cells exposed to DAPA, suggesting that DAPA stimulated the formation of autophagosomes and autolysosomes, leading to enhanced autophagic flux (Fig. 2C). To verify whether DAPA activated autophagy, we treated cells with rapamycin, known to induce autophagy [22], as a positive control.

DAPA alleviated hepatic accumulation in HFD mice and PA-stimulated HepG2 cells

We investigated the mechanisms by which DAPA inhibited hepatic triglyceride synthesis. Acetyl-CoA initiates fatty acid synthesis, which entails the incorporation of two-carbon units to elongate the fatty acid chain. The conversion of acetyl-CoA to malonyl-CoA and nicotinamide adenine dinucleotide phosphate (NADPH) is catalyzed by ACC, while the fatty acid chain is also extended to produce PA. Consequently, we investigated the primary enzymes and transcription factors involved in lipid metabolism within HepG2 cells. Treatment with DAPA (10 μM) resulted in a reduction of mRNA expression levels for ACC and FAS (Fig. 3A).

Thereafter, we investigated whether DAPA enhanced the degradation of fatty acids through β -oxidation. The mRNA levels of CPT1 α , a marker of β -oxidation, were significantly decreased with the addition of PA in HepG2 cells. In contrast, DAPA treatment increased mRNA levels of CPT1 α (Fig. 3B). Similarly, mRNA levels of LCAD were diminished by PA, whereas DAPA treatment reversed this effect, increasing LCAD mRNA levels (Fig. 3B). However, DAPA did not affect L-3-hydroxyacyl-CoA dehydrogenase alpha expression under the same conditions, suggesting that it protected hepatocytes from PA-induced lipotoxicity (Fig. 3B).

Given that Sirt1 serves as a central upstream regulator, both the reduction in fatty acid accumulation and the enhancement of fatty acid oxidation induced by DAPA appear to be downstream effects of Sirt1 activation. The transcription factor PPAR α directly influences multiple stages of hepatic lipid metabolism, including the activation of CPT1 α expression [23]. Given that DAPA upregulated CPT1 α expression, we assessed whether it also upregulated PPAR α expression. DAPA increased the mRNA levels of PPAR α in HepG2 cells treated with PA (Fig. 3B). This indicated that its protective effects were mediated, at least in

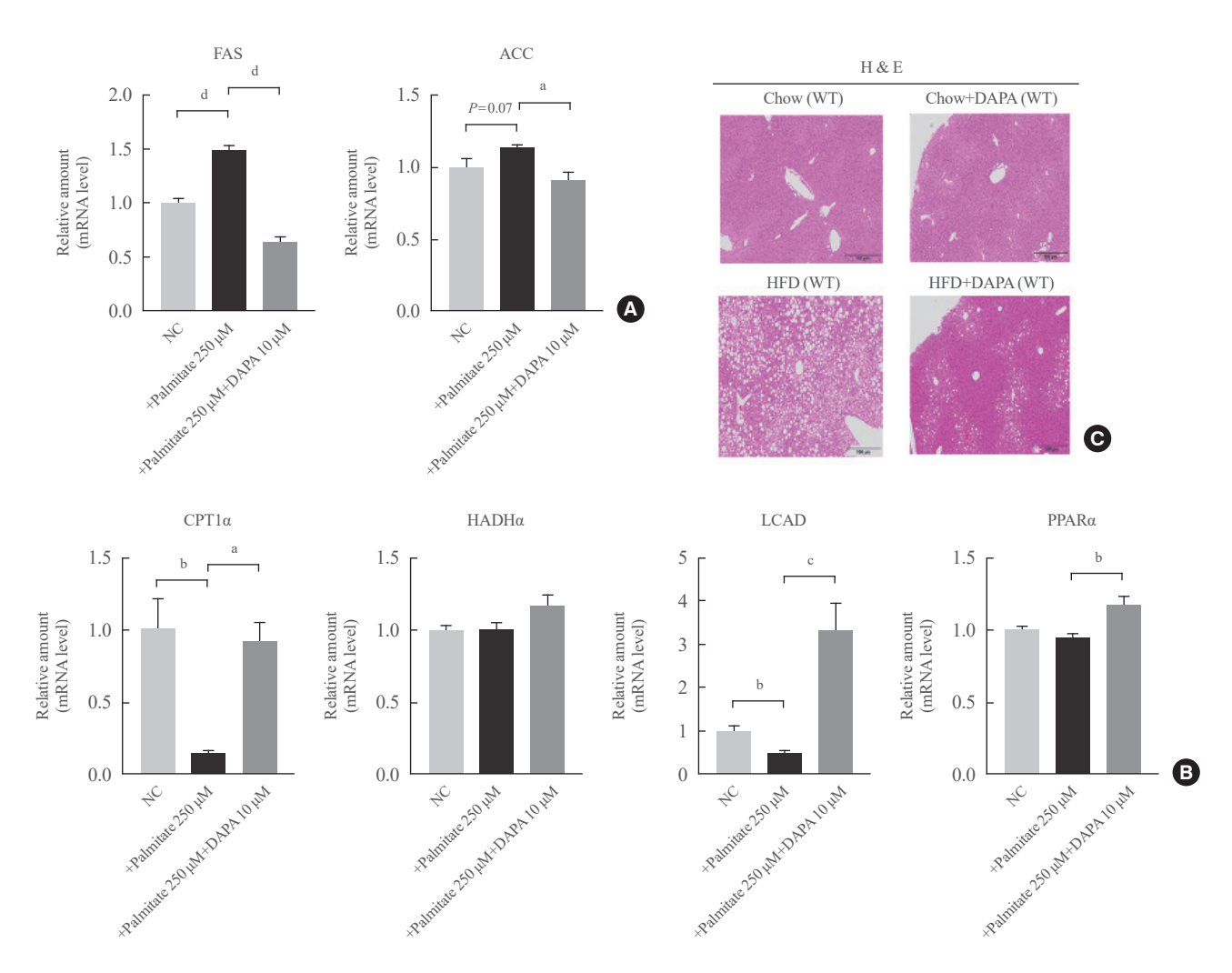


Fig. 3. Dapagliflozin (DAPA) reduces lipid accumulation and enhances lipid oxidation in HepG2 cells treated with palmitic acid. Histological analysis following H&E staining *in vivo* revealed that DAPA treatment mitigated hepatic steatosis by reducing intracellular lipid droplet formation. Cells are treated with 250 μM either in the absence or presence of DAPA. The levels of (A) fatty acid synthase (FAS) and acetyl-CoA carboxylase (ACC), as lipogenic enzymes, and (B) carnitine palmitoyltransferase 1α (CPT1α), hydroxyacyl-CoA dehydrogenase trifunctional multienzyme complex subunit alpha (HADHa), long-chain acyl-CoA dehydrogenase (LCAD), fatty oxidation genes, and peroxisome proliferator-activated receptor alpha (PPARα) are measured using quantitative reverse transcription polymerase chain reaction. The expression values of the target genes are normalized to those of the housekeeping gene glyceraldehyde-3-phosphate dehydrogenase. (C) Liver sections are processed with H&E staining (scale bar=100 μm). The data are presented as mean±standard error of the mean. NC, negative control; WT, wild-type; HFD, high-fat diet. Significance levels are indicated as aP <0.05; bP <0.01; cP <0.001; dP <0.0001.

part, through the upregulation of PPARα expression. To assess if DAPA reduced hepatic lipid accumulation *in vivo*, hepatic lipid accumulation was increased in the study groups. Histological analysis following H&E staining revealed that DAPA treatment mitigated hepatic steatosis by reducing intracellular lipid droplet formation (Fig. 3C).

DAPA promoted gluconeogenesis *in vitro* through the AMPK-Sirt1 signaling pathway

To evaluate if autophagy was triggered through the AMPK-Sirt1

pathway, RNA expression of Sirt1 and the protein levels of AMPK and Sirt1 were analyzed. The p-AMPK to AMPK ratio was increased in HepG2 cells treated with DAPA (Fig. 4B). Simultaneously, Sirt1 expression was increased (Fig. 4A). To explore the relationship between AMPK activation and autophagy triggered by DAPA, the AMPK inhibitor compound C was utilized to prevent AMPK phosphorylation in HepG2 cells. Compound C administration mitigated the DAPA-induced increase in Sirt1 expression (Fig. 4B). This indicated that the AMPK-Sirt1 axis was involved in the hepatic mechanism of action of DAPA.

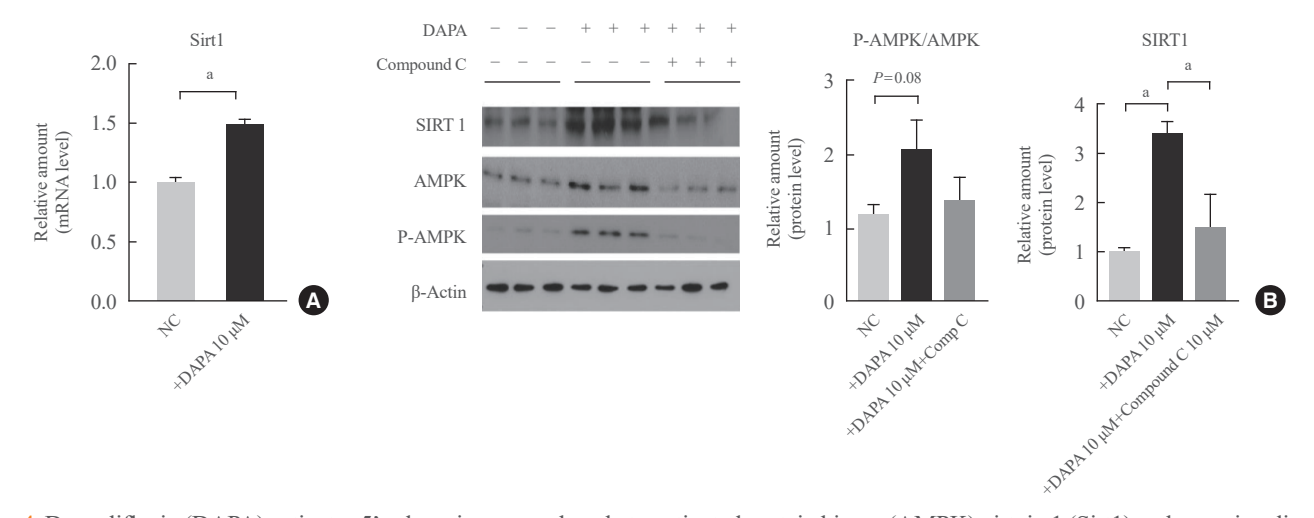


Fig. 4. Dapagliflozin (DAPA) activates 5'-adenosine monophosphate-activated protein kinase (AMPK)-sirtuin 1 (Sirt1) pathway signaling in HepG2 cells. (A) Sirt1 mRNA levels are upregulated in HepG2 cells treated with DAPA. The mRNA expression of the target gene is standardized against glyceraldehyde-3-phosphate dehydrogenase levels. (B) Western blot and corresponding densitometry analysis of p-AMPK and Sirt1 in hepatic cells. HepG2 cells are exposed to DAPA along with 10 µM compound C. Data are expressed as the mean±standard error of the mean. NC, negative control. Significance levels are indicated as ${}^{a}P < 0.05$.

DAPA increased hepatic glucose production and autophagic processes in mice fed a fat-rich diet

To assess the *in vivo* effects of DAPA on glucose regulation, we initiated a 12-week HFD regimen in mice aged 5 weeks. Thereafter, the mice were administered DAPA for 8 additional weeks. Notably, the average body weight was higher in the HFD Atg7 wild-type (WT) mice than in the chow diet Atg7 WT mice (Fig. 5A), regardless of dietary consumption. Fasting blood glucose (FBG) levels were evaluated, along with glucose tolerance, in week 25, insulin tolerance in week 26, and pyruvate tolerance in week 27. Significantly elevated FBG levels were observed in mice subjected to a far-rich diet. (Fig. 5B). The OGTT results were not significantly different between the HFD Atg7 WT group and the HFD+DAPA Atg7 WT group (Fig. 5C), indicating that DAPA did not enhance pancreatic beta-cell function by week 25. However, insulin sensitivity was notably improved in the two groups (Fig. 5D). Furthermore, PTT demonstrated significantly higher blood glucose levels in the HFD+DAPA Atg7 WT group than in the HFD Atg7 WT group (Fig. 5E), indicating enhanced hepatic gluconeogenesis in the former group.

To determine whether DAPA protected against lipid accumulation under our experimental conditions, we measured the serum levels of total cholesterol and triglycerides in the four groups. Both total cholesterol and triglyceride levels were increased in the HFD Atg7 WT group (Fig. 5F, G). However, DAPA treatment did not reduce the total cholesterol or triglyceride levels in these mice. The mice were euthanized at the end of the study (week 27), and liver tissues were analyzed. The data revealed higher PEPCK protein expression in the livers of HFD+DAPA Atg7 WT mice than in HFD Atg7 WT mice (Fig. 6). Additionally, transmission electron microscopy showed notable vacuolization and the presence of autophagosomes in the hepatocytes of HFD+DAPA Atg7 WT mice, with the proportion of autophagic vacuoles being markedly higher than in controls (Fig. 7). Collectively, these data demonstrated that DAPA treatment increased hepatic gluconeogenesis by stimulating autophagy.

DISCUSSION

This study investigated how DAPA, a SGLT2 inhibitor, affects hepatic glucose and lipid metabolism, focusing on its role in activating the AMPK-Sirt1 pathway and modulating autophagy. By examining both hepatic cells and HFD-fed mice, the study elucidated the previously unclear mechanisms by which DAPA activates gluconeogenesis and reduces lipid accumulation in the liver, which is a significant finding in understanding its role in managing obesity-related metabolic dysfunction.

SGLT2 inhibitors, such as DAPA, represent a novel category of oral medications designed to control blood sugar levels and manage type 2 diabetes mellitus [24]. Increased SGLT2 activity and expression have been detected in liver cells under elevated blood glucose conditions, leading to increased glucose reabsorption [25]. SGLT2 inhibitors, such as DAPA and empagliflozin, can increase hepatic gluconeogenesis and improve

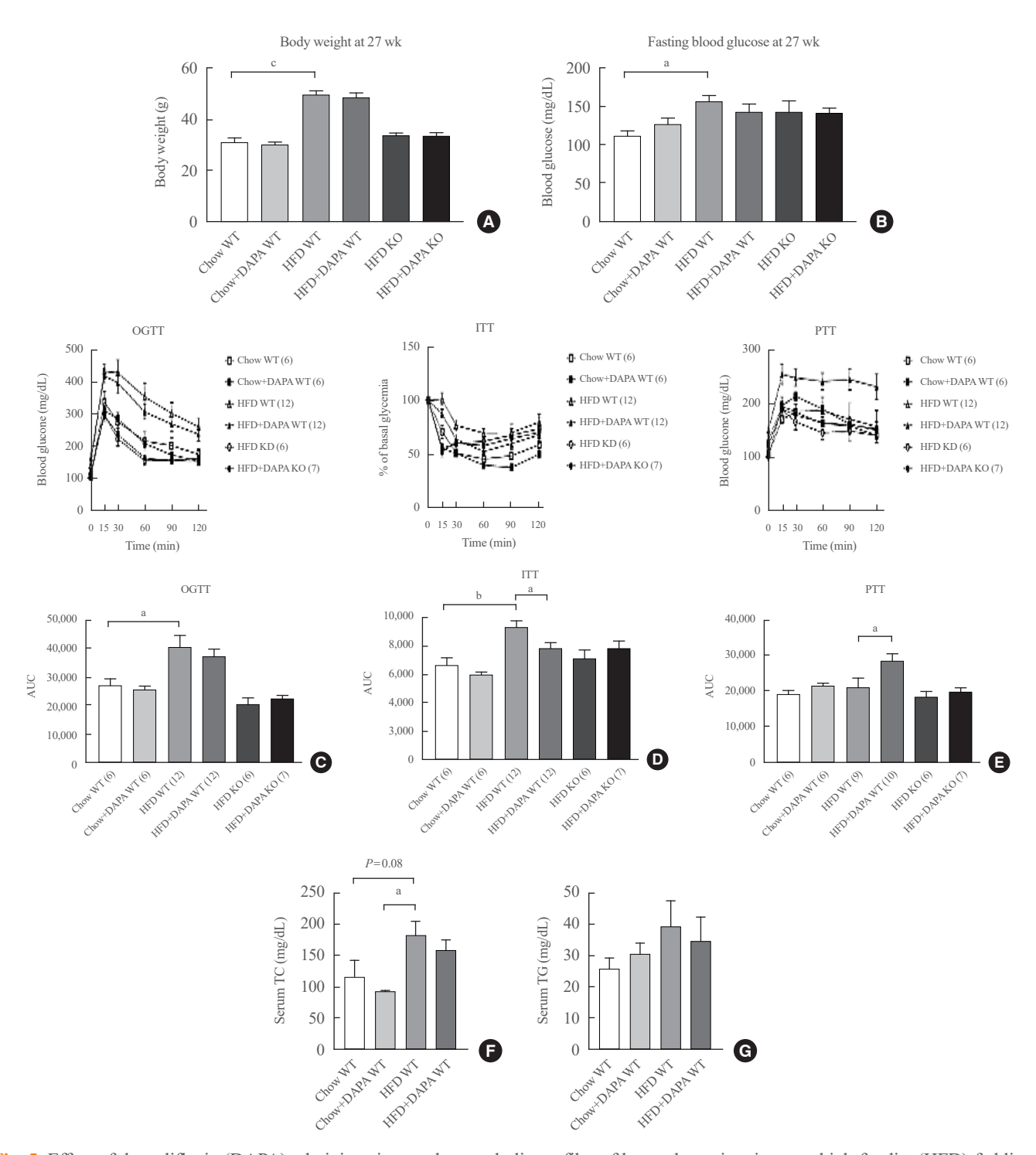


Fig. 5. Effect of dapagliflozin (DAPA) administration on the metabolic profiles of hyperglycemic mice on a high-fat diet (HFD)-fed liver-specific autophagy related 7 (Atg7) mice. (A) Influence of DAPA treatment on changes in body weight in Atg7 wild-type (WT) mice and Atg7 Δhep mice. (B) Fasting blood glucose levels are increased in Atg7 WT mice fed a HFD. (C) Results of the oral glucose tolerance test (OGTT) conducted at age 25 weeks indicate no differences between the groups (HFD-fed Atg7 WT mice and HFD+DAPA-fed Atg7 WT mice). (D) Results of insulin tolerance test (ITT) show improvement in insulin response in the DAPA-treated Atg7 WT mice. (E) Pyruvate tolerance test (PTT) conducted at age 27 weeks reveal increased blood glucose levels in the Atg7 WT mice treated with DAPA. (F) Triglyceride (TG). (G) Total cholesterol (TC). Data are presented as the mean±standard error of the mean. KO, knockout; AUC, area under the curve. Significance levels are indicated ^aP<0.05; ^bP<0.01; ^cP<0.0001.

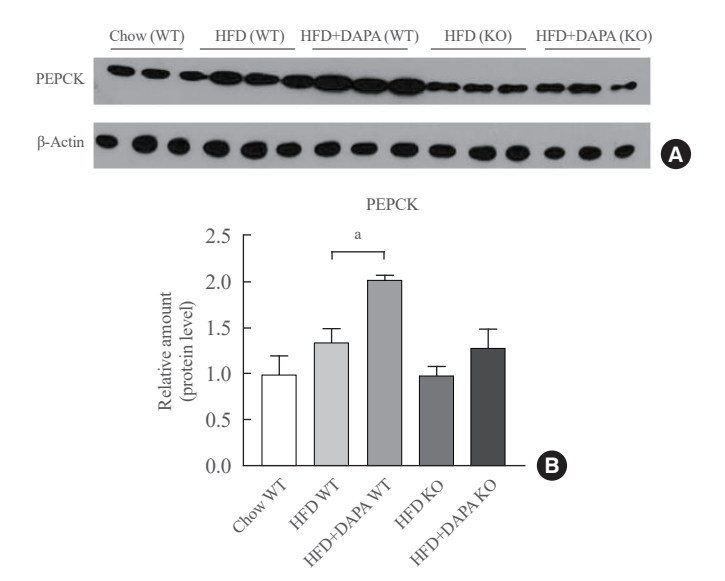


Fig. 6. Dapagliflozin (DAPA) treatment increases hepatic gluconeogenesis in vivo. (A) Western blot analysis is conducted to assess the protein expression levels of phosphoenolpyruvate carboxykinase (PEPCK), an essential gluconeogenic enzyme, in mice. (B) Densitometric analysis of Western blot results is performed to evaluate PEPCK expression in mice, with actin levels serving as a control. Densitometry analysis of PEPCK content is conducted with the ImageJ software (National Institutes of Health), normalizing the results to the control level. Data are presented as the mean±standard error of the mean. WT, wild-type; HFD, high-fat diet; KO, knockout. Significance levels indicated as ${}^{a}P < 0.05$.

metabolic and hepatic disorders [26-28]. However, the specific mechanisms linking these effects to glucose metabolism and liver function are poorly understood. Thus, understanding the precise mechanisms by which SGLT2 inhibitors enhance hepatic gluconeogenesis and mitigate diet-induced metabolic disorders is crucial.

SGLT2 is a sodium-glucose transporter predominantly found in the kidney's proximal convoluted tubules, but it has also been identified in other human tissues [29]. SGLT2 is expressed in immortalized HuS-E/2 human primary hepatocytes, HepG2 cell line human liver cancer cells, and liver tissues from mice [30-32]. The SGLT family, consisting of 12 members, presents an ongoing controversy regarding its expression signature in extrarenal tissues owing to the absence of specific antibodies [33]. However, previous studies have confirmed SGLT2 expression in liver cell lines and rat hepatic tissues [34]. Building on this, our study demonstrated that continuous treatment with DAPA significantly enhanced hepatic gluconeogenesis and reduced lipid deposition in mice given an HFD. This effect was correlated with the upregulation of gluconeogenic enzymes (e.g.,

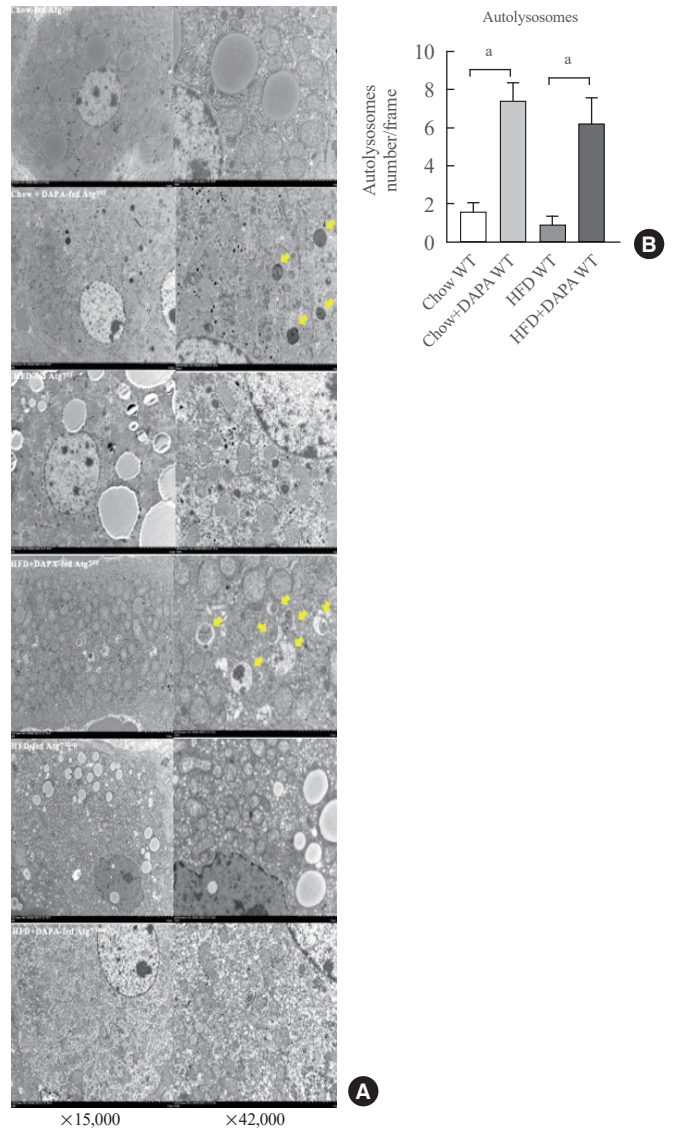


Fig. 7. Electron microscopy to analyze autophagosomes in the livers of mice that received dapagliflozin (DAPA) treatment. (A) Transmission electron microscopy shows significant vacuolization and autophagosomes in the hepatocytes of mice treated with DAPA. The arrows highlight the double membranes of the autophagosomes. (B) DAPA treatment substantially increases the formation of autophagic vacuoles in the mice livers. Data are presented as the mean±standard error of the mean. Atg7, autophagy related 7; HFD, high-fat diet; WT, wild-type. Significance levels defined as ${}^{a}P < 0.01$.

PEPCK and G6Pase), reduction in the expression of liver fat synthesis genes (e.g., FAS and ACC), and an increase in fatty acid oxidation genes (e.g., CPT1) in PA-stimulated HepG2 cells. Collectively, these results support that DAPA modulates hepatic gluconeogenesis and lipid metabolism through specific gene regulatory pathways, further implicating SGLT2 receptor

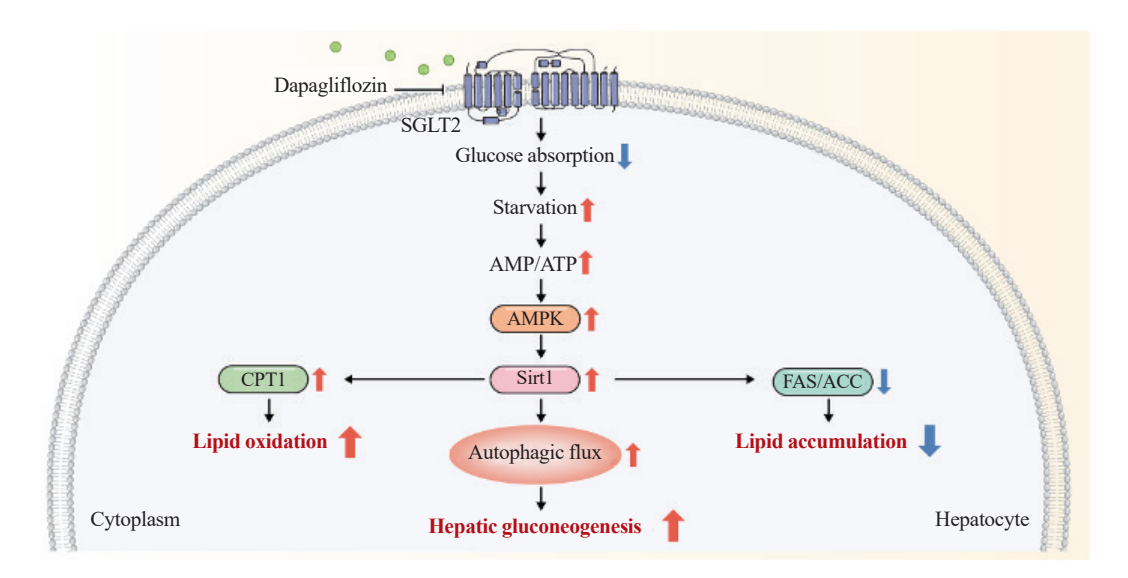


Fig. 8. Summary of the underlying mechanisms by which dapagliflozin induces hepatic gluconeogenesis and mitigates lipid accumulation. SGLT2, sodium-glucose cotransporter type 2; AMP, adenosine monophosphate; ATP, adenosine triphosphate; AMPK, 5'-adenosine monophosphate-activated protein kinase; CPT1, carnitine palmitoyltransferase 1; Sirt1, sirtuin 1; FAS, fatty acid synthase; ACC, acetyl-CoA carboxylase.

activity in these processes.

However, the specific mechanisms by which autophagy promotes gluconeogenesis remain to be elucidated. During periods of starvation, autophagy is believed to serve as a survival strategy, providing vital amino acids that facilitate gluconeogenesis in the liver [21,35]. Mice lacking autophagy due to Atg5 knockout generally succumb to hypoglycemic episodes occurring within 24 hours of birth [36]. Further, HFD mice with targeted deletion of Atg7 in the liver demonstrate enhanced insulin responsiveness and glucose tolerance relative to their WT littermates on the same diet [37]. Our findings demonstrate that DAPA treatment in HFD-fed mice leads to increased PEPCK expression and improved pyruvate tolerance, which is not observed in mice with a liver-specific deficiency in Atg7. This provides compelling evidence that DAPA promotes gluconeogenesis through autophagy. This is in line with previous findings that G6pc and Pck1 expressions are elevated in statin-treated primary hepatocytes but not in the liver cells of Atg7-deficient mice with liver-specific knockout [38]. In contrast, another study revealed that virus-induced enhanced expression of Atg7 lowered expression levels of rate-limiting enzymes related to gluconeogenesis in the liver tissue of mice [39]. However, this study did not verify whether Atg7 overexpression induced autophagy; therefore, whether the observed effects were attributable to autophagy induction remained uncertain.

AMPK serves as a key metabolic modulator, suppressing en-

ergy-demanding pathways while stimulating compensatory mechanisms to reestablish energy equilibrium [40]. AMPK is crucial to the activation of autophagy and SIRT1 activation as a reaction to different cellular stresses, including glucose deprivation [41,42]. Within hepatic tissues, the activation of AMPK modulates metabolism by enhancing catabolic processes (e.g., autophagy [43]) via SIRT1 activation [44] and fatty acid oxidation [45] while simultaneously inhibiting anabolic processes such as lipid biosynthesis [46]. Moreover, mammalian target of rapamycin, a key downstream effector of AMPK, exerts an inhibitory effect on autophagy activity [20]. Our study revealed that DAPA increased AMPK phosphorylation and subsequently upregulated SIRT1 expression in HepG2 cells, and this effect was counteracted by the AMPK-specific inhibitor compound C. This indicated that DAPA's influence on hepatic gluconeogenesis and its enhancement of hepatic steatosis was directly linked to AMPK activation (Fig. 8). These findings highlight the crucial involvement of the AMPK-SIRT1 signaling pathway in the activation of autophagy within the liver.

In this study, we observed no significant changes in the expression levels of glucose transporter 2 (GLUT2) and SGLT2 in HepG2 cells under DAPA treatment (Supplemental Fig. S1). However, independent of the expression levels of these transporters, previous studies using the SGLT2 inhibitor, canagliflozin, in the same cell line demonstrated a reduction in glucose uptake [31]. These findings support the hypothesis that

DAPA may act through a similar mechanism, leading to reduced glucose uptake in HepG2 cells.

The precise mechanism of SGLT2 inhibitor-induced gluconeogenesis remains under debate, with some studies suggesting an indirect effect through increased urinary glucose excretion, while others propose a direct impact on pancreatic alpha cells that stimulates glucagon secretion [14,15]. In our study, we observed a trend toward increased serum glucagon levels in the HFD+DAPA group compared to the HFD group, although the difference was not statistically significant (P=0.06) (Supplemental Fig. S2). This lack of statistical significance may be attributed to fasting conditions during the experimental design, as fasting is a known stimulus for glucagon secretion and likely elevated glucagon levels in both groups. Consequently, the fasting-induced increase in glucagon may have minimized the observable differences between the two groups. This suggests that while glucagon may play a role in the metabolic effects observed, its exact contribution to autophagy activation and hepatic gluconeogenesis remains uncertain. Recent studies have demonstrated that DAPA can exert direct effects on the liver. particularly under conditions of hepatic steatosis [34]. Similarly, our findings confirm that DAPA acts directly on HepG2 cells, where SGLT2 expression is observed (Supplemental Fig. S1). However, since the kidney remains the primary target of SGLT2 inhibitors, further clinical and structural studies are required to fully elucidate whether SGLT2 inhibitors have significant direct actions on the liver in humans.

One key strength of this study lies in its comprehensive approach, combining both laboratory settings and living organisms to assess the molecular pathways responsible for DAPA's effect on hepatic metabolism. The use of HepG2 hepatocellular carcinoma cells allowed us to explore specific intracellular processes, such as autophagy and expression levels of enzymes. Meanwhile, the use of Atg7-deficient mice with liver-targeted knockout and HFD-fed mouse models provided robust evidence for the function of autophagy in DAPA-induced metabolic changes. This combination of models strengthens the relevance of our findings across different biological systems, enhancing the generalizability of the results. Additionally, the detailed molecular analyses, including Western blotting, qRT-PCR, fluorescence microscopy, and transmission electron microscopy, offered strong mechanistic insights. By investigating the involvement of the AMPK-Sirt1 pathway, we not only demonstrated the pathways through which DAPA affected autophagy and metabolism, but also identified potential therapeutic targets for addressing hepatic steatosis and glucose dysregulation in metabolic diseases.

Despite these strengths, certain limitations warrant consideration. First, although HepG2 cells are a widely used model for studying liver metabolism, they may not fully replicate the complexity of human hepatic tissues. Therefore, further studies using primary hepatocytes or human liver biopsies would be necessary to confirm the clinical relevance of our findings. Additionally, although DAPA promoted hepatic gluconeogenesis in HFD-fed mice, it did not significantly alter serum cholesterol or triglyceride levels. This suggests that although DAPA can mitigate hepatic lipid accumulation, it may have limited effects on systemic lipid metabolism, warranting further investigation into its broader metabolic impacts. Moreover, our study primarily focused on the AMPK-Sirt1-autophagy axis. Although we identified autophagy as a key mediator of DAPA's action, the precise interplay among autophagy, glucose metabolism, and lipid oxidation requires further exploration. Future research can expand on these findings by investigating other metabolic pathways and regulatory mechanisms potentially involved in the effects of DAPA on hepatic metabolism.

In conclusion, DAPA enhanced hepatic gluconeogenesis and mitigated hepatic steatosis by increasing the key gluconeogenic enzymes PEPCK and G6Pase, decreasing the levels of the lipogenic enzymes FAS and ACC, enhancing the enzyme CPT1 involved in fatty acid oxidation, and stimulating autophagy. These positive outcomes appear to be facilitated by the activation of the AMPK-SIRT1 signaling pathway. Additionally, DAPA stimulates autophagy through the AMPK-SIRT1 pathway. Importantly, these results elucidated a novel mechanism by which DAPA alleviates hepatic steatosis, highlighting its role in augmenting hepatic gluconeogenesis through the SGLT2-mediated AMPK-SIRT1-autophagy pathway. This research offers new perspectives on the possible clinical uses of DAPA for non-alcoholic fatty liver disease by focusing on the modulation of intracellular autophagy in liver cells.

CONFLICTS OF INTEREST

No potential conflict of interest relevant to this article was reported.

ACKNOWLEDGMENTS

We thank Yonsei Advanced Imaging Center in cooperation with Carl Zeiss Microscopy, Yonsei University College of Medicine, for technical assistance. The authors wish to thank electron microscope core, Yonsei University College of Medicine, for technical assistance. This work was supported by the National Research Foundation of Korea (NRF) grant funded by Korea government (MSIT) (RS-2023-00209104) and a grant of the Korea Health Technology R&D Project through the Korea Health Industry Development Institute (KDHI), funded by the Ministry of Health & Welfare, Republic of Korea (HI23C0923). MID (Medical Illustration & Design), as a member of the Medical Research Support Services of Yonsei University College of Medicine, providing excellent support with medical illustration.

AUTHOR CONTRIBUTIONS

Conception or design: S.W.L., E.S.K. Acquisition, analysis, or interpretation of data: S.W.L., H.P., M.L., H.L., E.S.K. Drafting the work or revising: S.W.L. Final approval of the manuscript: E.S.K.

ORCID

Si Woo Lee https://orcid.org/0000-0001-8538-7416 Eun Seok Kang https://orcid.org/0000-0002-0364-4675

REFERENCES

- Zinman B, Wanner C, Lachin JM, Fitchett D, Bluhmki E, Hantel S, et al. Empagliflozin, cardiovascular outcomes, and mortality in type 2 diabetes. N Engl J Med 2015;373:2117-28
- 2. Neal B, Perkovic V, Mahaffey KW, de Zeeuw D, Fulcher G, Erondu N, et al. Canagliflozin and cardiovascular and renal events in type 2 diabetes. N Engl J Med 2017;377:644-57.
- Seo DH, Suh YJ, Cho Y, Ahn SH, Seo S, Hong S, et al. Effect of dapagliflozin in combination with lobeglitazone and metformin in Korean patients with type 2 diabetes in realworld clinical practice. Yonsei Med J 2022;63:825-33.
- Verma S, McMurray JJ. SGLT2 inhibitors and mechanisms of cardiovascular benefit: a state-of-the-art review. Diabetologia 2018;61:2108-17.
- Butler J, Hamo CE, Filippatos G, Pocock SJ, Bernstein RA, Brueckmann M, et al. The potential role and rationale for treatment of heart failure with sodium-glucose co-transporter 2 inhibitors. Eur J Heart Fail 2017;19:1390-400.
- Packer M, Anker SD, Butler J, Filippatos G, Pocock SJ, Carson P, et al. Cardiovascular and renal outcomes with empagliflozin in heart failure. N Engl J Med 2020;383:1413-24.
- 7. Petrie MC, Verma S, Docherty KF, Inzucchi SE, Anand I,

- Belohlavek J, et al. Effect of dapagliflozin on worsening heart failure and cardiovascular death in patients with heart failure with and without diabetes. JAMA 2020;323:1353-68.
- 8. Zelniker TA, Wiviott SD, Raz I, Im K, Goodrich EL, Bonaca MP, et al. SGLT2 inhibitors for primary and secondary prevention of cardiovascular and renal outcomes in type 2 diabetes: a systematic review and meta-analysis of cardiovascular outcome trials. Lancet 2019;393:31-9.
- McMurray JJV, Solomon SD, Inzucchi SE, Kober L, Kosiborod MN, Martinez FA, et al. Dapagliflozin in patients with heart failure and reduced ejection fraction. N Engl J Med 2019;381:1995-2008.
- Cannon CP, Pratley R, Dagogo-Jack S, Mancuso J, Huyck S, Masiukiewicz U, et al. Cardiovascular outcomes with ertugliflozin in type 2 diabetes. N Engl J Med 2020;383:1425-35.
- 11. Fitchett D, Zinman B, Wanner C, Lachin JM, Hantel S, Salsali A, et al. Heart failure outcomes with empagliflozin in patients with type 2 diabetes at high cardiovascular risk: results of the EMPA-REG OUTCOME® trial. Eur Heart J 2016;37:1526-34.
- 12. Dhillon S. Dapagliflozin: a review in type 2 diabetes. Drugs 2019;79:1135-46.
- 13. Ferrannini E, Muscelli E, Frascerra S, Baldi S, Mari A, Heise T, et al. Metabolic response to sodium-glucose cotransporter 2 inhibition in type 2 diabetic patients. J Clin Invest 2014; 124:499-508.
- 14. Bonner C, Kerr-Conte J, Gmyr V, Queniat G, Moerman E, Thevenet J, et al. Inhibition of the glucose transporter SGLT2 with dapagliflozin in pancreatic alpha cells triggers glucagon secretion. Nat Med 2015;21:512-7.
- Scafoglio C, Hirayama BA, Kepe V, Liu J, Ghezzi C, Satyamurthy N, et al. Functional expression of sodium-glucose transporters in cancer. Proc Natl Acad Sci U S A 2015;112: E4111-9.
- 16. Kurinami N, Sugiyama S, Yoshida A, Hieshima K, Miyamoto F, Kajiwara K, et al. Dapagliflozin significantly reduced liver fat accumulation associated with a decrease in abdominal subcutaneous fat in patients with inadequately controlled type 2 diabetes mellitus. Diabetes Res Clin Pract 2018;142:254-63.
- 17. Jojima T, Tomotsune T, Iijima T, Akimoto K, Suzuki K, Aso Y. Empagliflozin (an SGLT2 inhibitor), alone or in combination with linagliptin (a DPP-4 inhibitor), prevents steatohepatitis in a novel mouse model of non-alcoholic steatohepatitis and diabetes. Diabetol Metab Syndr 2016;8:45.

- 18. Xu Z, Hu W, Wang B, Xu T, Wang J, Wei D. Canagliflozin ameliorates nonalcoholic fatty liver disease by regulating lipid metabolism and inhibiting inflammation through induction of autophagy. Yonsei Med J 2022;63:619-31.
- 19. Hardie DG. AMP-activated protein kinase: maintaining energy homeostasis at the cellular and whole-body levels. Annu Rev Nutr 2014;34:31-55.
- 20. Kim J, Kundu M, Viollet B, Guan KL. AMPK and mTOR regulate autophagy through direct phosphorylation of Ulk1. Nat Cell Biol 2011;13:132-41.
- 21. Ezaki J, Matsumoto N, Takeda-Ezaki M, Komatsu M, Takahashi K, Hiraoka Y, et al. Liver autophagy contributes to the maintenance of blood glucose and amino acid levels. Autophagy 2011;7:727-36.
- Rangaraju S, Verrier JD, Madorsky I, Nicks J, Dunn WA, Notterpek L. Rapamycin activates autophagy and improves myelination in explant cultures from neuropathic mice. J Neurosci 2010;30:11388-97.
- Rakhshandehroo M, Knoch B, Muller M, Kersten S. Peroxisome proliferator-activated receptor alpha target genes. PPAR Res 2010;2010:612089.
- 24. Chaudhury A, Duvoor C, Reddy Dendi VS, Kraleti S, Chada A, Ravilla R, et al. Clinical review of antidiabetic drugs: implications for type 2 diabetes mellitus management. Front Endocrinol (Lausanne) 2017;8:6.
- 25. Nakano D, Akiba J, Tsutsumi T, Kawaguchi M, Yoshida T, Koga H, et al. Hepatic expression of sodium-glucose cotransporter 2 (SGLT2) in patients with chronic liver disease. Med Mol Morphol 2022;55:304-15.
- 26. Chiba Y, Yamada T, Katagiri H. Dapagliflozin, a sodium-glucose co-transporter-2 inhibitor, acutely reduces energy expenditure in brown adipose tissue via neural signals in mice. Yakugaku Zasshi 2018;138:945-54.
- 27. Trnovska J, Svoboda P, Pelantova H, Kuzma M, Kratochvilova H, Kasperova BJ, et al. Complex positive effects of SGLT-2 inhibitor empagliflozin in the liver, kidney and adipose tissue of hereditary hypertriglyceridemic rats: possible contribution of attenuation of cell senescence and oxidative stress. Int J Mol Sci 2021;22:10606.
- 28. Lee PC, Gu Y, Yeung MY, Fong CH, Woo YC, Chow WS, et al. Dapagliflozin and empagliflozin ameliorate hepatic dysfunction among chinese subjects with diabetes in part through glycemic improvement: a single-center, retrospective, observational study. Diabetes Ther 2018;9:285-95.
- 29. Uthman L, Baartscheer A, Schumacher CA, Fiolet JW, Kuschma MC, Hollmann MW, et al. Direct cardiac actions of

- sodium glucose cotransporter 2 inhibitors target pathogenic mechanisms underlying heart failure in diabetic patients. Front Physiol 2018;9:1575.
- Hawley SA, Ford RJ, Smith BK, Gowans GJ, Mancini SJ, Pitt RD, et al. The Na+/glucose cotransporter inhibitor canagliflozin activates AMPK by inhibiting mitochondrial function and increasing cellular AMP levels. Diabetes 2016;65: 2784-94.
- 31. Kaji K, Nishimura N, Seki K, Sato S, Saikawa S, Nakanishi K, et al. Sodium glucose cotransporter 2 inhibitor canagliflozin attenuates liver cancer cell growth and angiogenic activity by inhibiting glucose uptake. Int J Cancer 2018;142:1712-22.
- 32. Chiang H, Lee JC, Huang HC, Huang H, Liu HK, Huang C. Delayed intervention with a novel SGLT2 inhibitor NGI001 suppresses diet-induced metabolic dysfunction and non-alcoholic fatty liver disease in mice. Br J Pharmacol 2020;177: 239-53.
- 33. Wright EM, Loo DD, Hirayama BA. Biology of human sodium glucose transporters. Physiol Rev 2011;91:733-94.
- 34. Li L, Li Q, Huang W, Han Y, Tan H, An M, et al. Dapagliflozin alleviates hepatic steatosis by restoring autophagy via the AMPK-mTOR pathway. Front Pharmacol 2021;12:589273.
- 35. Mortimore GE, Hutson NJ, Surmacz CA. Quantitative correlation between proteolysis and macro- and microautophagy in mouse hepatocytes during starvation and refeeding. Proc Natl Acad Sci U S A 1983;80:2179-83.
- 36. Kuma A, Hatano M, Matsui M, Yamamoto A, Nakaya H, Yoshimori T, et al. The role of autophagy during the early neonatal starvation period. Nature 2004;432:1032-6.
- 37. Kim KH, Jeong YT, Oh H, Kim SH, Cho JM, Kim YN, et al. Autophagy deficiency leads to protection from obesity and insulin resistance by inducing Fgf21 as a mitokine. Nat Med 2013;19:83-92.
- 38. Wang HJ, Park JY, Kwon O, Choe EY, Kim CH, Hur KY, et al. Chronic HMGCR/HMG-CoA reductase inhibitor treatment contributes to dysglycemia by upregulating hepatic gluconeogenesis through autophagy induction. Autophagy 2015;11:2089-101.
- 39. Yang L, Li P, Fu S, Calay ES, Hotamisligil GS. Defective hepatic autophagy in obesity promotes ER stress and causes insulin resistance. Cell Metab 2010;11:467-78.
- 40. Ha J, Guan KL, Kim J. AMPK and autophagy in glucose/glycogen metabolism. Mol Aspects Med 2015;46:46-62.
- 41. Vingtdeux V, Giliberto L, Zhao H, Chandakkar P, Wu Q, Simon JE, et al. AMP-activated protein kinase signaling activation by resveratrol modulates amyloid-beta peptide me-



- tabolism. J Biol Chem 2010;285:9100-13.
- 42. Hou X, Xu S, Maitland-Toolan KA, Sato K, Jiang B, Ido Y, et al. SIRT1 regulates hepatocyte lipid metabolism through activating AMP-activated protein kinase. J Biol Chem 2008; 283:20015-26.
- 43. Alers S, Loffler AS, Wesselborg S, Stork B. Role of AMPK-mTOR-Ulk1/2 in the regulation of autophagy: cross talk, shortcuts, and feedbacks. Mol Cell Biol 2012;32:2-11.
- 44. Afshari H, Noori S, Zarghi A. A novel combination of metformin and resveratrol alleviates hepatic steatosis by activating autophagy through the cAMP/AMPK/SIRT1 signaling

- pathway. Naunyn Schmiedebergs Arch Pharmacol 2023; 396:3135-48.
- 45. Fernandez-Galilea M, Perez-Matute P, Prieto-Hontoria PL, Sainz N, Lopez-Yoldi M, Houssier M, et al. α-Lipoic acid reduces fatty acid esterification and lipogenesis in adipocytes from overweight/obese subjects. Obesity (Silver Spring) 2014;22:2210-5.
- 46. Zhou G, Myers R, Li Y, Chen Y, Shen X, Fenyk-Melody J, et al. Role of AMP-activated protein kinase in mechanism of metformin action. J Clin Invest 2001;108:1167-74.